scientific reports

Check for updates

OPEN

A colorimetric method to measure in vitro nitrogenase functionality for engineering nitrogen fixation

Lucía Payá-Tormo[1], Diana Coroian[1], Silvia Martín-Muñoz[1,2], Artavazd Badalyan[3], Robert T. Green[4], Marcel Veldhuizen[1], Xi Jiang[1,2], Gema López-Torrejón[1,2], Janneke Balk[4,5], Lance C. Seefeldt[3], Stefan Burén[1,2]✉ & Luis M. Rubio[1,2]✉

Biological nitrogen fixation (BNF) is the reduction of N_2 into NH_3 in a group of prokaryotes by an extremely O_2-sensitive protein complex called nitrogenase. Transfer of the BNF pathway directly into plants, rather than by association with microorganisms, could generate crops that are less dependent on synthetic nitrogen fertilizers and increase agricultural productivity and sustainability. In the laboratory, nitrogenase activity is commonly determined by measuring ethylene produced from the nitrogenase-dependent reduction of acetylene (ARA) using a gas chromatograph. The ARA is not well suited for analysis of large sample sets nor easily adapted to automated robotic determination of nitrogenase activities. Here, we show that a reduced sulfonated viologen derivative (S_2V^{red}) assay can replace the ARA for simultaneous analysis of isolated nitrogenase proteins using a microplate reader. We used the S_2V^{red} to screen a library of NifH nitrogenase components targeted to mitochondria in yeast. Two NifH proteins presented properties of great interest for engineering of nitrogen fixation in plants, namely NifM independency, to reduce the number of genes to be transferred to the eukaryotic host; and O_2 resistance, to expand the half-life of NifH iron-sulfur cluster in a eukaryotic cell. This study established that NifH from *Dehalococcoides ethenogenes* did not require NifM for solubility, [Fe-S] cluster occupancy or functionality, and that NifH from *Geobacter sulfurreducens* was more resistant to O_2 exposure than the other NifH proteins tested. It demonstrates that nitrogenase components with specific biochemical properties such as a wider range of O_2 tolerance exist in Nature, and that their identification should be an area of focus for the engineering of nitrogen-fixing crops.

Although almost 80% of the atmosphere is composed of nitrogen gas (N_2), crop productivity in modern agriculture is limited by biologically available nitrogen such as oxidized (*e.g.* NO_3^-) or reduced (*e.g.* NH_4^+) species[1]. Crop yield is increased using synthetic N-based fertilizers that are costly both economically and ecologically, due to the consumption of non-renewable energy resources, production of greenhouse gasses, and water and air pollution[2]. On the other hand, biological nitrogen fixation (BNF) is performed by selected prokaryotes (bacteria and archaea), named diazotrophs for their capacity to grow using N_2 as the sole N source[3]. A diverse range of diazotrophs are found in Nature and can be classified according to their lifestyle as free living, symbiotic (mainly bacteria living within root nodules of legume plants, including pulse crops), and those that live in associative or endophytic relationship with other organisms. Three biotechnological approaches are currently being explored to reduce the application of N-based fertilizers to cereal crops by enhancing their access to BNF[4,5]. In the first strategy, bacteria naturally associated with cereals are engineered to improve their colonization ability, N_2-fixing capabilities or NH_3 release. In the other two strategies, the plants are instead genetically engineered to either generate new symbiotic relationships between the non-legume plant and N_2-fixing bacteria, thus mimicking the legume-rhizobium natural symbiosis, or by direct transfer of the prokaryotic N_2 fixation genes into the plant, to create a crop capable of fixing N_2 without the requirement for symbiotic associations. Both approaches are

[1]Centro de Biotecnología y Genómica de Plantas, Universidad Politécnica de Madrid, Instituto Nacional de Investigación y Tecnología Agraria y Alimentaria (INIA-CSIC), Campus de Montegancedo UPM, Crta M-40 km 38 Pozuelo de Alarcón, 28223 Madrid, Spain. [2]Departamento de Biotecnología-Biología Vegetal, Escuela Técnica Superior de Ingeniería Agronómica, Alimentaria y de Biosistemas, Universidad Politécnica de Madrid, 28040 Madrid, Spain. [3]Department of Chemistry and Biochemistry, Utah State University, Logan, UT, USA. [4]Department of Biochemistry and Metabolism, John Innes Centre, Norwich NR4 7UH, UK. [5]School of Biological Sciences, University of East Anglia, Norwich NR4 7TJ, UK. ✉email: stefan.buren@upm.es; lm.rubio@upm.es

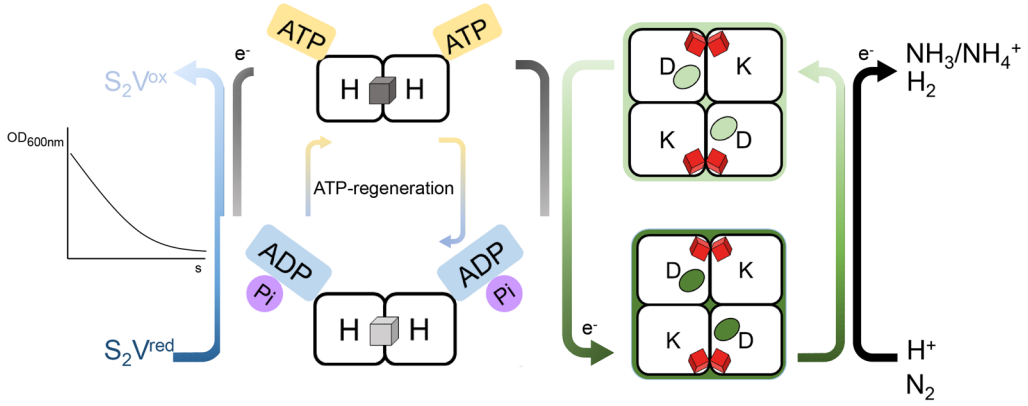

Figure 1. Schematic overview of nitrogenase activity and activity determination using S_2V^{red}. The flow of electrons from S_2V^{red} to protons (H^+) or N_2 via NifH and NifDK is shown. At NifDK, H_2 or NH_4^+ (the dominating form at pH 7) is produced. ATP is regenerated from ADP and phosphocreatine by the action of creatine phosphokinase. Nitrogenase activity is determined by measuring the decrease in absorbance at 600 nm.

ambitious and challenging. The new symbiotic relationship requires molecular signaling between the bacteria and plants to avoid an immune response, the formation of a nodule-like structure with a low-O_2 environment and the productive exchange of nutrients between the plant and the bacteria. On the other hand, the transfer of the N_2 fixation capability is complicated by the estimated number of required genes (ca. 10–20), the sensitivity of their products towards O_2, the need to perform time consuming functional validations, and difficulty to troubleshoot pathway engineering in plants[6].

Diazotrophs harbor a protein complex called nitrogenase that converts nitrogen (N_2) into ammonia (NH_3) in an intricate process requiring a large amount of energy in the form of ATP and low potential electrons[7]. Nitrogenase has two protein components: an $\alpha_2\beta_2$ heterotetrameric dinitrogenase formed by the *nif*rogen *f*ixation (*nif*) *nifD and nifK* gene products, and a *nifH*-encoded homodimeric dinitrogenase reductase. During N_2 to NH_3 reduction, one NifH homodimer binds to each αβ half of the NifDK protein and, in an ATP-dependent reaction, transfers the electrons needed to break the N_2 triple bond[8]. Nitrogenase requires a minimum of 16 ATP molecules and 8 electrons to convert one molecule of N_2 into two molecules of NH_3[9]. The electrons are funneled through three [Fe-S] clusters, starting at a [Fe_4S_4] cluster bridging the two subunits of NifH, via the P-cluster ([Fe_8S_7]) and finally to the iron molybdenum cofactor (FeMo-co, [$MoFe_7S_9C$-(*R*)-homocitrate]). The latter two clusters are located at each αβ half of the NifDK heterodimer[9]. All three metalloclusters are extremely O_2-sensitive, which makes engineering nitrogenase in plants especially challenging.

The activity of nitrogenase can be determined in vitro (*e.g.* using pure protein components), in vivo (*e.g.* in free-living cells) or in situ (*e.g.* bacteria associated to plants) using various techniques. One direct method is the quantitative measurement of the ammonia produced using its natural substrate N_2[10], or by ^{15}N enrichment or ^{15}N natural abundance methods[11–13]. Furthermore, nitrogenase activity can be indirectly measured as nitrogenase can also reduce protons into H_2[14,15], but also other double- and triple-bonded substrates such as acetylene, nitrite, nitrous oxide, and azide[16]. This promiscuity is often used by researchers to study nitrogenase in the laboratory. The most-used method is the acetylene reduction assay (ARA) in which acetylene is reduced to ethylene, which is detected using gas chromatography[17–20]. However, the ARA has several drawbacks. Firstly, the number of samples that can be measured is low due to the manual work involved. The manual steps include exchange of the gas phase in the reaction vial using inert argon to prevent N_2 reduction; injection of acetylene to start the reaction; incubation in a water-bath, injection of EDTA or NaOH to stop the reaction; and finally injection of gas from the vial headspace into the gas chromatograph. Secondly, acetylene reduction cannot be easily monitored in real time, and only the end concentration of ethylene after a defined time is determined. This second limitation of the ARA was recently overcome by the development of a viologen-based electron donor to nitrogenase[21]. In that method a reduced sulfonated viologen derivative (1,1′-bis(3-sulfonatopropyl)-4,4′-bipyridinium radical, hereafter referred to as S_2V^{red}) replaces the function of sodium dithionite (DTH) as electron donor to NifH in vitro. Upon nitrogenase activity and turnover, this deeply violet-colored substrate is converted into an oxidized colorless form (S_2V^{ox}) with greatly diminished absorbance at 600 nm (Fig. 1). The decrease in absorbance over time is therefore linear with nitrogenase activity. However, the exposure of the violet-colored S_2V^{red} to an oxidizing agent such as O_2 (or other reactive oxygen species), or to other natural electron acceptors, will lead to its conversion into the oxidized and colorless form (S_2V^{ox}), limiting the use of S_2V^{red} to in vitro measurements under anaerobic conditions.

In this work, we have adapted the S_2V^{red} method to determine nitrogenase activity in 96-well microtiter plates with the aim to screen distinct NifH variants expressed in the mitochondria of the yeast *Saccharomyces cerevisiae* for functionality. The development of screening methods allows us to find Nif components with improved properties desirable for its expression in plant organelles. We demonstrate that: (1) the results obtained using S_2V^{red} are in accordance with those seen when using the standard ARA; (2) the method is compatible with NifH proteins originating from different prokaryotic origins; and (3) many samples and assay conditions can

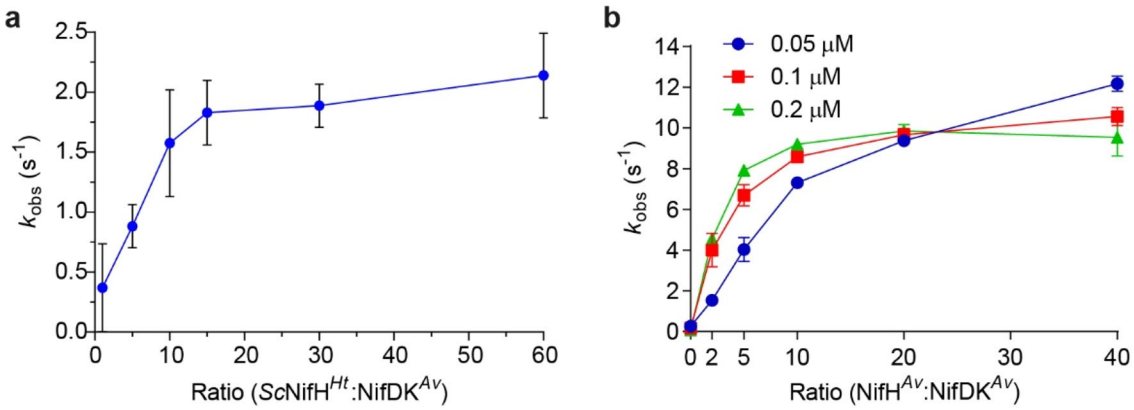

Figure 2. Adaptation and optimization of S_2V^{red} for nitrogenase activity determination using 96-well microtiter plates. **(a)** Nitrogenase activity (k_{obs} (s^{-1})) measured in a cuvette using *Sc*NifH^{Ht} and NifDK^{Av} at 0–60 × molar ratios in reactions containing 0.4 μM NifDK^{Av}. Mean and SD is shown. $n = 2$ technical replicates. **(b)** Nitrogenase activity (k_{obs} (s^{-1})) measured in a 96-well microtiter plate using NifH^{Av} and NifDK^{Av} at 0–40 × molar ratios in reactions containing 0.05 μM (blue dots), 0.1 μM (red squares) or 0.2 μM (green triangles) NifDK^{Av}. Mean and SD is shown. $n = 2$ technical replicates.

be tested in parallel. We used S_2V^{red} to determine the activity of nine distinct NifH proteins. NifH variants that were compatible with the *Azotobacter vinelandii* NifDK were tested for NifM dependency and O_2 sensitivity, two properties of importance to engineer nitrogenase in crop plants.

Results

Adaptation and use of S_2V^{red} for screening and activity determination of NifH proteins using 96 well microtiter plates. To confirm that S_2V^{red}-dependent electron donation to nitrogenase is not unique to NifH isolated from *A. vinelandii* (hereafter denoted as NifH^{Av}), as previously shown[21], but is also suitable for functional screening of novel NifH variants, we combined the *Hydrogenobacter thermophilus* NifH protein previously isolated from *S. cerevisiae*[22] with NifDK^{Av}. NifH variants expressed in yeast are hereafter denoted as *Sc*NifH^{Xx} where *Sc* and *Xx* indicates *S. cerevisiae* and the species from which the NifH sequence was obtained, respectively. Robust, although slower, oxidation of S_2V^{red} was observed using *Sc*NifH^{Ht} compared to NifH^{Av} (Fig. 2). This was expected from the lower specific activity of *Sc*NifH^{Ht} when combined with NifDK^{Av} determined by ARA in previous studies[22]. We next tested functionality of the S_2V^{red} assay using NifH^{Av} and NifDK^{Av} in 96 well microtiter plates sealed in the glove box (95% N_2 and 5% H_2). Several NifDK concentrations (0.05–0.2 μM) and NifH to NifDK molar ratios (2x-40x) were tested to identify conditions that provided a robust and linear rate constant (k_{obs}) over an extended time-period (to facilitate sample preparations and plate handling), and that minimized the amount of NifH and NifDK proteins required for the assay. Supplementary Fig. S1 shows the decrease in absorbance over time under the tested experimental conditions. As expected, higher NifDK concentrations resulted in a faster S_2V^{red} oxidation (Supplementary Fig. S1d). Supplementary Figure S2 shows the corresponding k_{obs} variation over time. The fast S_2V^{red} oxidation observed at high NifDK concentration resulted in lower k_{obs} (Supplementary Fig. S2c), presumably because the concentration of S_2V^{red} was already suboptimal by the time the plate was being scanned (after sealing in the glove box and transfer to the plate reader). The maximum activity observed under the conditions tested here (k_{obs} of ca. 12 s^{-1}) was obtained when the mixture contained 2 μM NifH^{Av} and 0.05 μM NifDK^{Av} (corresponding to a NifH:NifDK ratio of 40) (Fig. 2b), and was almost identical to that reported when performed under argon atmosphere and using cuvettes[21]. Importantly, the decrease in absorbance was linear under these conditions for more than 10 min (Supplementary Fig. S1b) ($R^2 = 0.9997$, $t_1 = 1$ to $t_2 = 10$ min), which provided sufficient time for microtiter plate preparation, transfer and reading. These experimental conditions were therefore implemented for subsequent use of S_2V^{red}.

Solubility screening of NifH variants targeted to the mitochondria of yeast. To obtain proof-of-concept of S_2V^{red} suitability to quickly screen the function of engineered Nif proteins, we used a library of 35 mitochondria-targeted NifH proteins in yeast (Supplementary Tables S1 and S2). The bulk of the NifH variants originated from a library that had previously been tested in *Nicotiana benthamiana*[22]. The NifH variants were expressed as N-terminally TwinStrep (TS)-tagged proteins with a Cox4 mitochondria targeting signal[23,24]. The purpose of the TS-tag was to enable equal detection of the distinct NifH variants and their subsequent isolation using Strep-tag affinity chromatography (STAC). The NifH proteins were co-expressed with NifM, NifU and NifS using galactose inducible promoters. NifM has been proposed to be necessary for proper folding of the NifH polypeptide[25], whereas NifU and NifS provide NifH with its [Fe_4S_4] cluster[7]. All the accessory proteins originated from *A. vinelandii* and were equipped with a Su9 leader sequence[24,26]. The functionality of the Cox4 and the Su9 sequences for mitochondrial targeting of each respective protein in yeast has been shown previously[22,27,28].

With the assumption that Nif components must accumulate as soluble proteins to be relevant for engineering nitrogenase in eukaryotes, we first tested the NifH variant solubility. Accumulation of *Sc*NifH^{Xx} variant

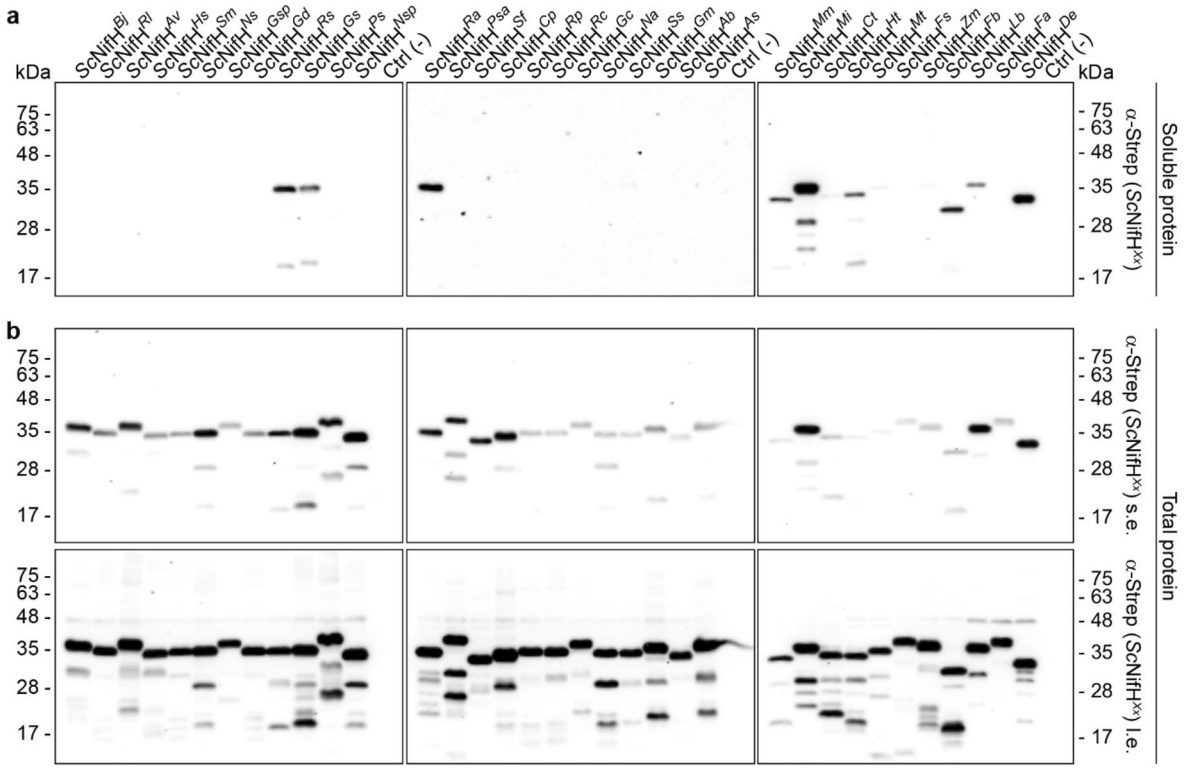

Figure 3. NifH library solubility screening. **(a,b)** Presence of *Sc*NifH^{Xx} (see Supplementary Table S2 for full species names) in soluble (a) and total (b) protein extracts was determined using antibodies detecting the TwinStrep-tag (α-Strep). Two different exposure times (s.e., short exposure (above) and l.e., long exposure (below)) are shown for the analysis of total extracts.

polypeptides, co-expressed with NifM, NifU and NifS, was confirmed by immunoblot analysis of total protein extracts (Supplementary Fig. S3). Nine out of the 35 *Sc*NifH variants were detectable at noticeable levels in soluble extracts (Fig. 3). These nine NifH variants originated from *Roseiflexus* sp. (strain RS-1), *H. thermophilus* (strain TK-6), *Geobacter sulfurreducens* (strain PCA), *Ruminococcus albus* (strain SY3), *Methanothermobacter marburgensis* (strain Marburg), *Methanocaldococcus infernus* (strain ME), *Firmicutes* bacterium CAG:536, *Leptolyngbya boryana* (strain Dg5) and *Dehalococcoides ethenogenes* (strain 195). Of these nine, the NifH variants from *H. thermophilus*, *M. marburgensis* and *M. infernus* were shown to be soluble in a previous study from our group[22].

Isolation and activity measurements of soluble *Sc*NifH variants. Three of the nine soluble *Sc*NifH variants (from *H. thermophilus*, *M. marburgensis* and *M. infernus*) had already been purified in our laboratory[22]. The remaining *Sc*NifH proteins (together with *Sc*NifH^{Ht} that was reisolated for further work described in this study) were isolated using STAC under anaerobic conditions (Fig. 4a–c, Supplementary Fig. S4). The yield varied from 9–35 mg *Sc*NifH per 100 g cell paste for six of the variants (Table 1), in line to what was previously reported for *Sc*NifH^{Mm} and *Sc*NifH^{Mi}. Only *Sc*NifH^{Lb} was isolated at much lower level. This variant was excluded from further analysis. These *Sc*NifH proteins all presented color and an UV–vis absorbance spectrum characteristic of [Fe–S] cluster containing proteins (Fig. 4d, Supplementary Fig. S5). Iron quantification suggested that six *Sc*NifH variants had a similar amount of bound [Fe-S] cluster as NifH^{Av} purified from its native host[29] (Table 1), while *Sc*NifH^{Mi} and *Sc*NifH^{Mm} were isolated with much lower Fe content.

We then performed nitrogenase assays with the different *Sc*NifH proteins using S_2V^{red} as the electron donor to NifH, and NifDK^{Av} as its electron acceptor (Fig. 4e). Three variants, namely those originating from *H. thermophilus* (*Sc*NifH^{Ht}), *G. sulfurreducens* (*Sc*NifH^{Gs}) and *D. ethenogenes* (*Sc*NifH^{De}), accelerated S_2V^{red} oxidation when the *Sc*NifH:NifDK^{Av} ratio was increased, which is expected from a functional and NifDK^{Av}-compatible NifH variant. These *Sc*NifH proteins showed acetylene reduction activities consistent with those obtained using S_2V^{red} (Fig. 4e,f). Interestingly, *Sc*NifH^{Rs} (and to some extent *Sc*NifH^{Ra}) could act as reductase for NifDK^{Av} during ARA (*i. e.* when using DTH as electron donor), but not in the S_2V^{red} assay (Fig. 4f). This divergence could potentially originate from different reduction potential requirements among the NifH variants, as S_2V^{red} has a potential of – 0.40 V vs Normal Hydrogen Electrode (NHE)[21] and DTH has a potential of – 0.66 V vs NHE[30]. Whether this discrepancy indicates a different mechanism or requirement for NifH^{Rs} activity remains to be investigated in future studies.

Inhibition of *Sc*NifH by O_2. The NifDK^{Av} compatible *Sc*NifH variants were assayed for their sensitivity to O_2, which represents a major barrier to engineer nitrogenase in plants. As S_2V^{red} itself is oxidized by O_2, and

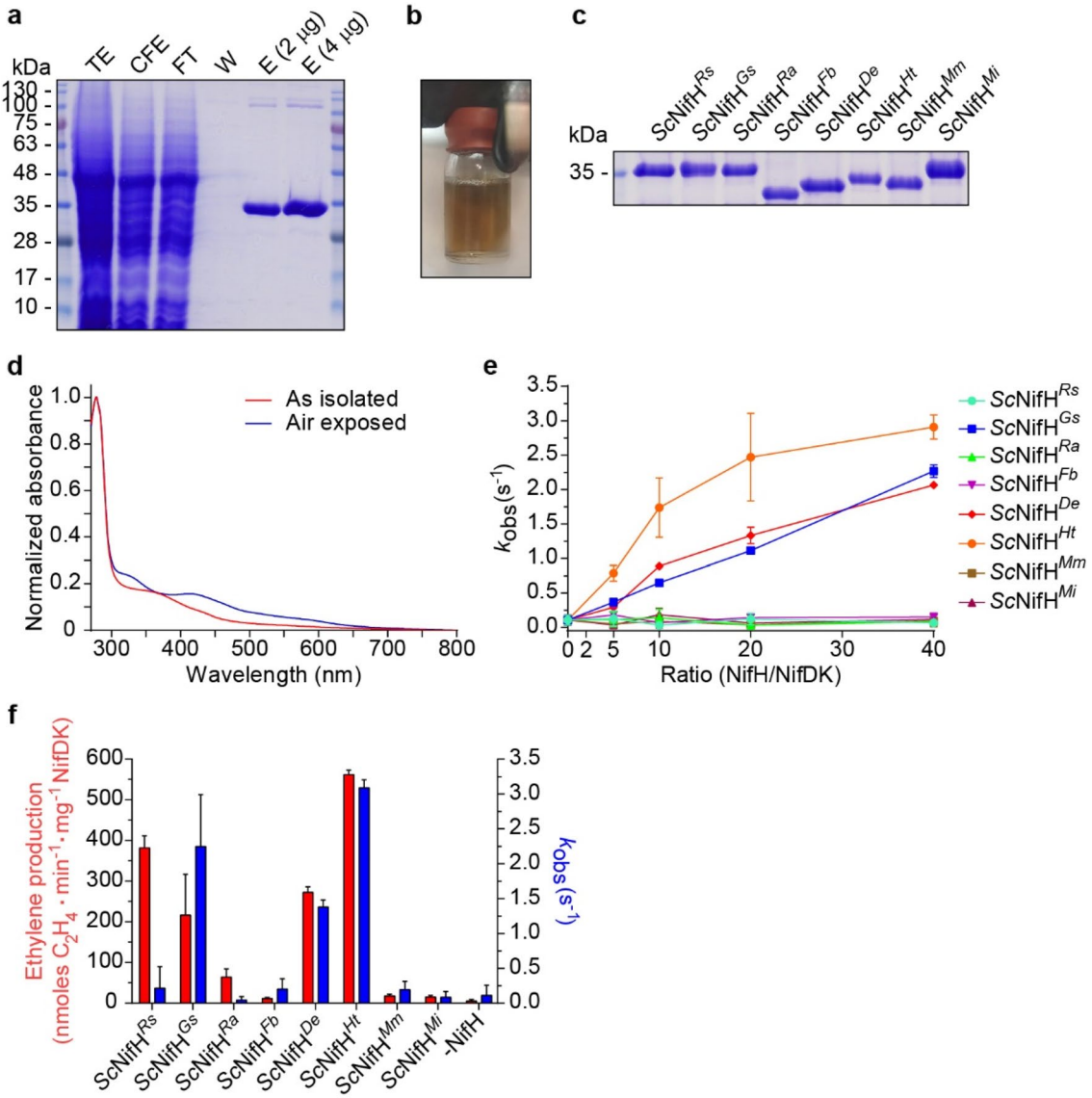

Figure 4. Functionality of soluble *Sc*NifH^{Xx} candidates. **(a)** Example of the STAC-purification process of *Sc*NifH^{Xx} (represented here by *Sc*NifH^{Ra}). TE, total extract after yeast cell breakage using high-pressure homogenizer; CFE, cell-free extract after centrifugation and filtering of the TE; FT, flow-through after passing the CFE through the STAC column; W, wash fraction; E, final concentrated and desalted elution fraction. **(b)** Example of concentrated and desalted elution fraction (here represented by *Sc*NifH^{Fb}, Supplementary Fig. S4d), 7 ml final volume. **(c)** Coomassie staining of soluble *Sc*NifH^{Xx} variants isolated from soluble yeast extracts using STAC. Approximately 3 µg protein was loaded per sample. More details of the purification process are shown in Supplementary Fig. S4. The uncropped Coomassie stained gel is shown in Fig. S11. **(d)** Example of UV–vis absorption spectra of as-isolated and air-exposed *Sc*NifH^{Xx} (represented here by *Sc*NifH^{Ra}). **(e)** Nitrogenase activities with increasing concentrations of *Sc*NifH^{Xx} proteins using S_2V^{red} as electron donor and NifDK^{Av} as electron acceptor. Mean and SD is shown. $n = 2$ technical replicates. **(f)** Nitrogenase activities using *Sc*NifH^{Xx} proteins and NifDK^{Av} (at a 40:1 molar ratio) as determined by ARA (ethylene production, left Y-axis, red bars) or using S_2V^{red} ($k_{obs}^{(s-1)}$, right Y-axis, blue bars). Mean and SD is shown. $n = 3$ technical replicates (ARA) and $n = 4$ (S_2V^{red}).

O_2-destruction of the $[Fe_4S_4]$-cluster at NifH is extremely fast (the half-life of NifH upon O_2 exposure is reported to be about 30–45 s)[31,32], we were not able to design an experiment using S_2V^{red} to study the effect of O_2 on the activity. We therefore measured the *Sc*NifH variants capacity to support acetylene reduction upon exposure to O_2 following a previously reported method[31]. In short, DTH present in the buffer of the isolated *Sc*NifH protein was first removed using a desalting column inside an anaerobic glove box. The *Sc*NifH protein was then added to anaerobic buffer in a glass vial containing argon in the headspace (representing $t = 0$). Then, O_2 was injected into the headspace to a final concentration of 20% and the vial was incubated with rigorous shaking. At distinct time points, *Sc*NifH was extracted using a Hamilton syringe and transferred to an open vial containing anaerobic buffer supplemented with DTH to quench the O_2. Finally, NifDK^{Av} and an ATP-regenerating mixture was added

NifH variant	Fe atoms per NifH dimer	Yield (mg NifH per 100 g cells)
Roseiflexus sp.	3.11 ± 0.42	35.2
G. sulfurreducens	2.52 ± 0.40	11.8
R. albus	3.22 ± 1.24	23.0
D. ethenogenes	1.93 ± 0.004	8.5
D. ethenogenes (-NifM)	1.97 ± 0.44	14.6
Firmicutes bacterium	2.79 ± 0.20	23.0
H. thermophilus (reisolated in this work)	2.06 ± 0.04	20.2
M. marburgensis (purified in previous work)	0.74 ± 0.41	2.86
M. infernus (purified in previous work)	0.87 ± 0.09	19.9
L. boryana	–	–
A. vinelandii (purified from *A. vinelandii*)	3.19 ± 0.05	–

Table 1. Iron content per NifH dimer and purification yield for all soluble NifH variants purified from yeast. Iron content shows mean and standard deviation (n = 2 technical replicates).

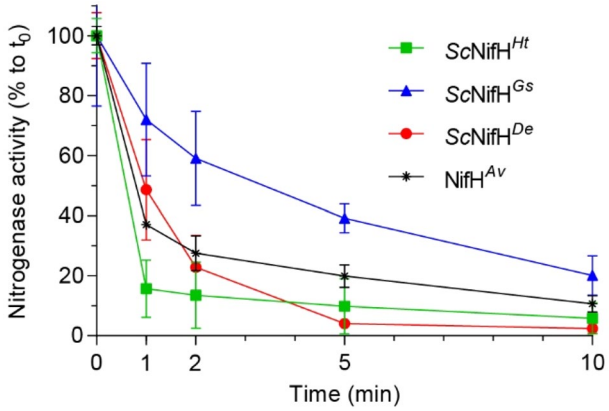

Figure 5. Sensitivity of *Sc*NifH^{Xx} variants to O_2. Nitrogenase activity of *Sc*NifH^{Ht} (green squares), *Sc*NifH^{Gs} (blue triangles) and *Sc*NifH^{De} (red dots) was measured by ARA upon exposure to oxygen. NifH^{Av} was used as NifH control protein (black stars). The molar ratio of NifH:NifDK^{Av} was 40:1. Nitrogenase activity is shown in relation to the activity obtained prior to oxygen exposure at t_0 (for *Sc*NifH^{Ht} 532 ± 30 units (nmol ethylene formed per min and mg of NifDK^{Av}), for *Sc*NifH^{Gs} 159 ± 37 units, for *Sc*NifH^{De} 188 ± 14 units and for NifH^{Av} 1673 ± 51 units). Mean and SD is shown. *n* = 5 or 6 technical replicates.

before the standard ARA. Similar to the *Klebsiella pneumoniae* NifH protein[31], the half-life for NifH^{Av} was less than one minute (Fig. 5). While *Sc*NifH^{Ht} and *Sc*NifH^{De} presented similar kinetics regarding the inhibition from O_2 exposure as NifH^{Av}, the *Sc*NifH^{Gs} retained 50% activity for about 4 min, and about 25% activity after 10 min O_2 exposure.

NifM-dependency for *Sc*NifH solubility and functionality. Co-expression of the *A. vinelandii nifM* gene with *nifH*^{Av} is required for the accumulation of functional NifH^{Av} protein in the mitochondria of *S. cerevisiae*[33]. Several of the NifH sequences in this study were selected because of the absence of a *nifM* orthologue in the organism's genome. To test whether NifM was required for the solubility of the eight *Sc*NifH variants, we compared their accumulation in total and soluble protein extracts when co-expressed with NifU^{Av} and NifS^{Av}, but not NifM^{Av}, in yeast. Surprisingly, six of the eight *Sc*NifH variants (*Roseiflexus* sp., *R. albus*, *M. marburgensis*, *M. infernus*, *Firmicutes* bacterium, and *D. ethenogenes*) showed no obvious decrease in solubility when NifM^{Av} was absent (Fig. 6a). To test whether functionality could be affected although solubility was not, we isolated *Sc*NifH^{De} from the yeast strain not expressing NifM^{Av} (Fig. 6b, Supplementary Fig. S6a). The UV–vis spectrum suggested no apparent difference in [Fe-S] cluster content (Supplementary Fig. S6b), and the specific activity was similar to *Sc*NifH^{De} protein isolated from cells co-expressing NifM^{Av} (Fig. 6c).

Seven of our eight *Sc*NifH variants contained a proline residue at the site corresponding to Pro^{259} (when including the methionine) in *A. vinelandii* (Fig. 6d, Supplementary Fig. S7), which is thought to be the target of NifM prolyl isomerase activity[25]. The NifH protein from *Firmicutes* bacterium is shorter and terminates before this proline. Interestingly, the only genome of the eight selected NifH variants that contained a gene with high similarity to NifM^{Av} was *G. sulfurreducens* (Supplementary Table S2). *Sc*NifH^{Gs} was also the variant that was least soluble when NifM^{Av} was not co-expressed (Fig. 6a). The only other protein that showed reduced solubility in the absence of NifM^{Av} was *Sc*NifH^{Ht}. The genome of *H. thermophilus* harbors a gene encoding a hypothetical protein

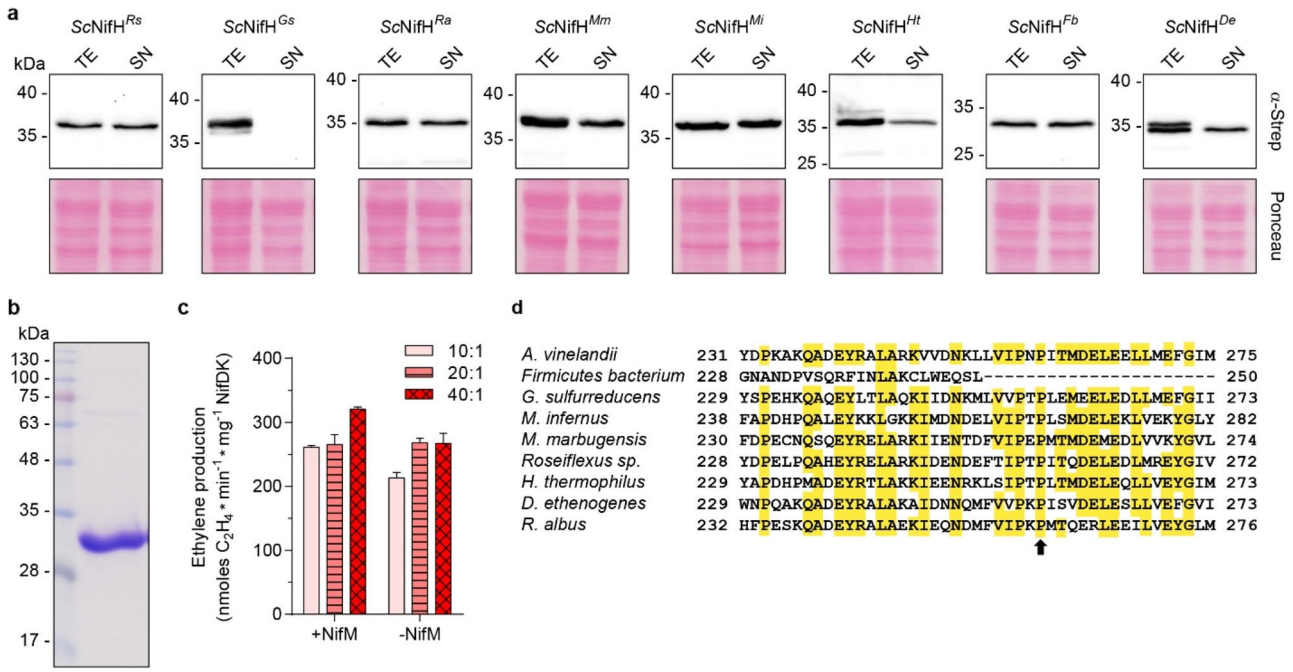

Figure 6. Effect of NifM^{Av} on *Sc*NifH^{Xx} solubility and functionality. **(a)** Immunoblot analysis of the levels of *Sc*NifH^{Xx} variants in total yeast extracts (TE) and the soluble fractions (SN) when expressed in the absence of NifM^{Av}. The uncropped immunoblots and membranes are shown in Fig. S12. **(b)** *Sc*NifH^{De} isolated from yeast cells not expressing NifM^{Av}. The uncropped Coomassie stained gel is shown in Fig. S13. **(c)** Comparison of the specific activity of *Sc*NifH^{De} isolated from yeast cells expressing (+NifM) or not expressing NifM (−NifM) using ARA. The molar ratio of *Sc*NifH^{De} to NifDK^{Av} is indicated. Mean and SD is shown. $n=2$ technical replicates. **(d)** Alignment of NifH^{Av} with the eight *Sc*NifH^{Xx} variants analyzed in (**a**). The C-terminal domain containing Pro^{259} in NifH^{Av} (indicated by a black arrow) proposed to be the target of NifM action is shown. The full sequence alignment can be found in Supplementary Fig. S7.

with a PPIC-type PPIASE domain and with moderate similarity to NifM^{Av}. Interestingly, isolation of the soluble population of *Sc*NifH^{Ht} that was produced in the absence of NifM^{Av} resulted in a protein with identical specific activity to *Sc*NifH^{Ht} isolated from yeast cells co-expressing of NifM^{Av} (Supplementary Fig. S8). Therefore, the direct action of NifM with regards to NifH is not clear and to some extent in disagreement with the published literature[7], and should be the topic of future studies.

Discussion

The transfer of prokaryotic nitrogenase activity into cereals could generate crops suited to grow well under limited nitrogen fertilizer. Although there are excellent reports on engineering of nitrogenase in heterologous (non-N_2-fixing) bacterial hosts[34–40], our experience is that it is very difficult to directly translate and transfer that knowledge to a eukaryotic system and expect comparable results, even in a relatively simple, unicellular eukaryote such as yeast[41]. A major challenge arises from the extremely complex biochemical requirements of the nitrogenase enzyme and its stepwise maturation involving several inter-dependent gene products[7]. Additionally, from a metabolic point of view, nitrogenase requires high levels of energy and reducing power in an environment that is low in O_2 to protect its metalloclusters from oxidative damage.

In this study we have developed an important part of the nitrogenase engineering process, namely the analysis of NifH protein functionality in a high throughput assay. While the ARA is very precise, it requires training to generate consistent results, it is rather time-consuming and would be difficult to scale up for screening large numbers of samples and/or conditions. We optimized the S_2V^{red} assay and showed that it fulfilled many of our main objectives, most importantly to be fast and simple to use, to require a lower amount of purified proteins (corresponding to about half of that used in the ARA as the reaction volume is smaller), and to not depend on expensive or sophisticated equipment. We also believe that this method is easily adaptable to automated robotic systems as the reactions are performed in microtiter plates. In addition, the S_2V^{red} assay has two important advantages over the ARA. Firstly, activities can be monitored in real-time, which means that it is possible to directly study the effect of various effector molecules or reaction components on nitrogenase functionality. Secondly, the reduction potential of S_2V^{red} (used as the electron donor to NifH) is much closer to that of ferredoxin or flavodoxin, the physiological reductants of nitrogenase[42,43] than DTH. NifF for example, a flavodoxin in the diazotrophic free-living model-bacteria *A. vinelandii* donating electrons to NifH, harbors a flavin mononucleotide (FMN) cofactor with a redox potential in the semiquinone/hydroquinone state of − 0.483 V vs NHE[44]. The corresponding potentials for S_2V^{red} is − 0.40 V vs NHE, compared to − 0.66 V vs NHE for DTH[21,30]. However, it is important to note that other reported flavodoxins and ferredoxins have lower reduction potentials, for example

flavodoxin in *A. chroococcum* (− 522 mV)[45] and ferredoxin in *A. vinelandii* (− 619 mV)[46], and that S_2V^{red} would not be a suitable electron donor to study nitrogenases requiring such strong reductants. Whether this could explain the lack of nitrogenase activity when combining *Sc*NifH^{Rs} and *Sc*NifH^{Ra} with NifDK^{Av} in the S_2V^{red} is not clear, as it is also possible that other steric or charge factors prelude productive electron transfer from S_2V^{red} to these NifH variants. Other important drawback with using S_2V^{red} is that it is not commercially available, and that it cannot be used directly with yeast extracts as it is effectively oxidized by unknown molecule(s) in the lysate (data not shown). Therefore, Nif proteins must be purified prior to the activity assay. Solving this limitation would further expand the use of the S_2V^{red}.

Regarding the functional assessment of Nif proteins expressed in yeast and plants, we have observed that many of the essential Nif components have poor solubility, especially NifH and NifB[22,24,27,47]. This is critical as the structural components (NifH and NifDK) are needed at very high levels during nitrogen fixation. In N_2-fixing *A. vinelandii* for example the NifH concentration within the cell can reach up to 100 μM[48], whereas in *K. oxytoca* about 40% of the total protein is NifHDK[49]. For this, a simple protein solubility study is always the first experiment to perform before initiating more complex analyses[22,27]. From the 35 mitochondrial-targeted NifH variants expressed in this study, we obtained nine that were soluble in yeast mitochondria. The phyla from where these nine NifH variants originated were diverse, and so was their mechanisms of nutrition and relationship to oxygen. The only common factor we could observe was a bias towards coming from thermophilic organisms, as has been observed and discussed previously in works from our laboratory[22,24,27].

To expand the analysis of these soluble NifH variants and to see if we could identify properties that would facilitate their functionality in future crops, we tested two aspects that are sought after for eukaryotic nitrogenase engineering; 1) simplification of the nitrogenase genetic machinery by minimizing the number of genes needed to transfer, and 2) identification of Nif components with better functionality in an environment containing oxygen. In this work, that meant (1) the identification of a NifH variant that did not depend on NifM for solubility and functionality, and (2) one NifH variant whose [Fe_4S_4] cluster was more resistant towards O_2.

Although NifM is just one protein, each gene fewer to transfer will make the engineering of nitrogenase in plants less complex. When the *K. pneumoniae* NifH protein was expressed in *Escherichia coli* in the absence of NifM, the protein was much less stable and completely inactive[50]. This was in agreement with the low levels of NifH^{Kp} polypeptide and dinitrogenase reductase activity detected in *nifM*$^{-}$ strains of the native host[51]. Work in yeast has shown that NifM co-expression was required for homodimer formation and polypeptide stability of *Rhizobium meliloti* NifH[52], and in tobacco NifM was required to prevent NifH aggregation in the mitochondria[53]. While not many studies have investigated how NifM acts on NifH, sequence analysis suggests NifM to be a member of the rotamase family (PF00639) containing a PPIC-type PPIASE domain[54]. Prolyl isomerases (also known as peptidylprolyl isomerases or PPIases) are enzymes that accelerate protein folding by catalyzing the *cis–trans* isomerization of prolyl peptide bonds. This annotation is consistent with work identifying Pro^{259} in NifH from *A. vinelandii* as the prime target for NifM action[25]. In this work, seven of the final eight variants contained a proline residue at the site corresponding to Pro^{259} in *A. vinelandii*. The only exception was NifH from *Firmicutes bacterium*, but this protein was significantly shorter than the other NifH variants and therefore lacking this proline. However, the only two NifH variants that showed NifM-dependent solubility (*Sc*NifH^{Gs} and *Sc*NifH^{Ht}) corresponded to those that originated from organisms containing genes with some similarity to *nifM*^{Av}. Therefore, our work suggests that presence of a *nifM* homologue in the organism genome is a better indicator of NifM-dependency than presence of a proline at a site corresponding to Pro^{259} in *A. vinelandii*.

Equally important is the identification of more O_2-resistant nitrogenase components, as O_2-sensitivity is likely to be the major barrier to overcome to obtain a functional plant nitrogenase[5]. Active NifH could be expressed in the cytosol of anaerobically cultured yeast, while only the mitochondria could produce active protein under aerobic conditions[33]. This has been explained by the low O_2 concentration in the mitochondria of actively respiring cells. Whether it is possible to obtain similarly O_2-depleted conditions in plant mitochondria is not known. One scenario would be to limit nitrogenase expression to plant cells in hypoxic niches[55]. In any case, the identification of more O_2-tolerable nitrogenase components would be a breakthrough for the engineering of nitrogenase in crops. In this regard, we were surprised to see increased resistance towards O_2 by NifH from *G. sulfurreducens*. As all NifH proteins contain a [Fe_4S_4] cluster, we assumed that the variants tested in this study would also show similar O_2-susceptibility. Whether the [Fe_4S_4] cluster in *Sc*NifH^{Gs} is less exposed, or whether it is stabilized by other means, is not known but these are interesting questions for future work. Importantly, this study shows that Nif proteins with better properties for expression in eukaryotic cells exist in Nature, and that their identification could pave the way for the engineering of N_2 fixing crops.

Materials and methods

NifH library design and assembly. The majority of the *nifH* genes originated from a previously published gene set[22]. To this *nifH* library the genes for expression of NifH originating from *L. boryana*, *Frankia alni* and *D. ethenogenes* were added. All yeast codon-optimized DNA sequences and their corresponding protein products can be found in Supplementary Table S2. The *nifH* genes originating from the previously published gene set[22] were amplified as *cox4-ts-nifH* gene fusions by PCR using primers #2584 (5′-AATTTTTGAAAATTCGAATTC CTCTTGACCATGCTTTCAC-3') and #2585 (5′-GAAGAATTGTTAATTAAGAGCTCGGGGAAATTCGAG CTGG-3′). These primers include 15 bp overhangs complementary to the pESC-HIS yeast expression plasmid (#217451, Agilent Technologies) when digested with *Sac*I and *Eco*RI, and allowed for the insertion by an exonuclease and ligation-independent (ELIC) method[56]. The *nifH* genes originating from *L. boryana*, *F. alni* and *D. ethenogenes* were amplified using primers #2902 (5′-CACAATTTGAAAAAGGATCCATGTCTGACGAAA ACATTAG-3′) and #2903 (5′-GGAAATTCGAGCTGGTCACCTTAAGCACCAGCCTTAGCCA-3′), #2904 (5′-CACAATTTGAAAAAGGATCCATGAGACAAATTGCTTTCTA-3′) and #2905 (5′-GGAAATTCGAGC

TGGTCACCTTAAGCAACAGCAGCAGCCT-3′), #2906 (5′-CACAATTTGAAAAAGGATCCATGAGAA AGGTTGCTATTTA and #2907 (5′-GGAAATTCGAGCTGGTCACCTTAAGAAATAACACCAAATT-3′), respectively. The amplified *nifH* sequences were inserted by ELIC into pESC-HIS (*cox4-ts-nifH*$^{B.\ japonicum}$) digested with *Nco*I and *BstE*II, replacing the *B. japonicum nifH* gene with *nifH* from *L. boryana*, *F. alni* or *D. ethenogenes*. The gene encoding for mitochondria-targeted SU9-NifM^{Av} was amplified from plasmid pN2XJ165[22] using primers #2478 (5′- CTCTACAAATCTATCTCTCTCGAGATGGCCTCCACTCGTG-3′) and #2479 (5′- ATTATG GAGAAACTCGAGTTAACCATGTGCTAAGTTTTCC-3′) and inserted into pESC-TRP (#217453, Agilent Technologies) digested with *Xho*I by ELIC. The pESC-URA plasmid for expression of mitochondria-targeted Su9-NifU^{Av} and Su9-NifS^{Av} has been previously described[33]. All DNA digestions were performed using enzymes from New England Biolabs. PCR amplifications were carried out using Phusion Hot Start II High-Fidelity DNA Polymerase (ThermoFisher Scientific). ELIC products with their corresponding digested target vectors were transformed using a molar ratio 1:4 (vector:insert) into chemically competent *E. coli* DH5α and selected on solid LB (Lysogenic broth) media supplemented with appropriate antibiotics. Plasmid preparations were performed using Qiaprep Spin Miniprep kit (QIAGEN) and correct cloning was confirmed by Sanger sequencing (Macrogen). Plasmids were transformed into *S. cerevisiae* W303-1a (*MAT*a *leu2-3,112 trp1-1 can1-100 ura3-1 ade2-1 his3-11,15*) according to the lithium acetate method[57], and selected and grown in synthetic drop-out medium with the appropriate auxotrophic selection[24].

Expression analysis and solubility screening of *Sc*NifH^{Xx} variants. Small-scale yeast protein extracts were prepared from yeast grown in galactose induction media as previously described[24]. The YeastBuster protein extraction reagent (Merck) was used to prepare total and soluble yeast protein extracts. First, galactose-induced yeast was pelleted for 10 min at 3000×*g*. YeastBuster mixture supplemented with 25 µg/ml DNAse I and 1 mM phenyl-methylsulfonyl fluoride (PMSF) was added to the yeast pellets at a ratio of 9 µl per OD × ml in Eppendorf tubes, and then incubated on a Eppendorf shaker for 20 min at room temperature to lyse the cells. This sample was then divided in two equal parts. For total extracts, the resulting YeastBuster lysate was added to 2 × Laemmli buffer at a 1:1 (v/v) ratio. For soluble extracts, the YeastBuster lysate was centrifuged in a benchtop centrifuge at maximum speed for 20 min at 4 °C before the supernatant was added to 2 × Laemmli buffer at a 1:1 (v/v) ratio. Both samples were prepared for SDS-PAGE by heating for 5 min at 95 °C.

Following SDS-PAGE, proteins were either stained using Coomassie brilliant Blue R-250 (Sigma) or transferred to nitrocellulose membranes (Protran Premium 0.45 µm, GE Healthcare) membranes for immunoblotting. Nitrocellulose membranes were stained with Ponceau S (Sigma) to ensure equal loading control and successful transfer. The membranes were blocked with 5% non-fat milk in TBS-T (20 mM Tris–HCl pH 7.5, 150 mM NaCl, 0.02% Tween-20) for 1 h at room temperature before incubation with primary antibodies overnight at 4 °C. Polyclonal antibodies detecting NifM^{Av} (used at 1:2,000 in 5% BSA), NifU^{Av} (used at 1:2000 in 5% BSA) and NifS^{Av} (used at 1:1,000 in 5% BSA), were raised against purified preparations of the corresponding *A. vinelandii* proteins (generated in house). Strep-tag II antibody ("Strep-MAB", IBA Lifesciences, 1:2000 in 5% BSA) was used for detection of all *Sc*NifH^{Xx} variants. Secondary antibodies (Sigma) were diluted 1:20,000 in TBS-T supplemented with 2% non-fat milk and incubated for 2 h at room temperature. Membranes were developed using enhanced chemiluminescence and images were recorded digitally (iBright FL1000, ThermoFisher).

***S. cerevisiae* growth and NifH variants purification.** The growth of yeast cultures, galactose-induced Nif expression and STAC-purification of soluble *Sc*NifH^{Xx} variants followed the procedure previously described[27]. Cell pellets from 4 l fermenters stored in liquid N_2 (typically 200–220 g) were resuspended in lysis buffer (100 mM Tris–HCl pH 8.8, 200 mM NaCl, 10% glycerol, 2 mM DTH, 1 mM PMSF, 1 µg/ml leupeptin, 5 µg/ml DNAse I) at a ratio of 1:2 (w/v) inside an anaerobic glovebox (Coy Laboratories). Total extracts (TE) were prepared by lysis of the cell suspensions under anaerobic atmosphere using an EmulsiFlex-C5 homogenizer (Avestin Inc.) operating at 20,000 psi. The TE was transferred to centrifuge tubes equipped with sealing closures (Beckman Coulter) and centrifuged at 50,000×*g* for 1 h at 4 °C (Avanti J-26 XP). The supernatant was filtered using filtering cups with a pore size of 0.2 µm (ThermoFisher), rendering cell-free extract (CFE) of soluble proteins that was loaded at 2.5 ml/min into a 5 ml Strep-Tactin XP column (IBA LifeSciences) attached to an ÄKTA FPLC (GE Healthcare) at O_2-levels below 1 ppm in anaerobic chambers operating at 16 °C (MECAPLEX or MBraun). The column was washed overnight using about 120 ml wash buffer (100 mM Tris–HCl pH 8.0, 200 mM NaCl, 10% glycerol, 2 mM DTH). Strep-Tactin XP column-bound proteins were eluted with 15 ml washing buffer supplemented with 50 mM biotin (IBA LifeSciences). The elution fraction was concentrated using centrifugal filters with 30 kDa cutoff (Amicon, Millipore), loaded into PD-10 desalting columns (GE Healthcare) equilibrated with wash buffer to remove biotin and DTH, and then used to UV–Vis absorption spectrum analysis (see section below). The desalted eluate was supplemented with 2 mM DTH, further concentrated using centrifugal filters and finally snap-frozen as protein pellets in cryovials (Nalgene) and stored in liquid N_2.

Protein quantification, UV–Vis absorption spectrum and iron measurements. The concentrations of purified *Sc*NifH^{Xx} variants were measured using the BCA protein assay (Pierce) in combination with iodoacetamide to eliminate the interfering effect of DTH[58]. *Sc*NifH^{Xx} UV–Vis absorption spectra were recorded after removal of the DTH from the protein samples. The DTH-free protein samples were further diluted in wash buffer and transferred to Q6 spectroscopy cuvettes with sealing closures. Absorption (280 nm to 800 nm) was recorded using a UV-2600 spectrophotometer (Shimadzu). For recording of the air exposed *Sc*NifH^{Xx} samples, the sealing closure was removed, and the protein sample was carefully exposed to air using a pipette equipped with a gel loading tip. Iron content of as isolated *Sc*NifH^{Xx} preparations and NifH^{Av} (used as $[Fe_4S_4]$ containing control protein) was determined by atomic absorption using a graphite furnace installed in a ContrAA 800

AAS Spectrometer (Analytik Jena). Protein samples were denatured using 30% HNO_3 for 1 h at 80 °C, and then diluted in metal-free ultra-pure water to a final concentration of 1.5% HNO_3. Twenty µl of diluted sample were used for iron measurement according to the following protocol: I) sample drying at 100 °C for 25 s, II) pyrolysis at 350 °C for 10 s, III) pyrolysis at 1100 °C for 20 s, IV) gas adaptation at 1100 °C for 5 s, V) atomization at 2000 °C for 10 s, and finally VI) cleaning of the furnace at 2500 °C for 5 s. Each sample was measured in triplicates. An absorbance wavelength of 248.327 nm was selected for specific iron measurement. For quantification, an iron standard curve from 0 to 20 parts per billion (ppb) was prepared from a 1000 parts per million (ppm) iron standard solution (Inorganic Ventures). The spectrometer protocol was set up and controlled using the ASpect CS software (version 2.2.2.0).

Nitrogenase activity determination by S_2V^{red} assay in cuvette. Nitrogenase activity of *Sc*NifH^{Ht} expressed in yeast mitochondria and isolated by STAC[22] was determined following a recently described spectrophotometric method[21]. Activity assays were performed in cuvette (600 µl final reaction volume) in the presence of ATP regenerating mixture (6.7 mM $MgCl_2$, 5 mM ATP, 30 mM phosphocreatine, 0.2 mg/ml creatine phosphokinase, 1.3 mg/ml bovine serum albumin (BSA) in 100 mM MOPS pH 7.0) and 0.5 mM 1,1′-bis(3-sulfonatopropyl)-4,4′-bipyridinium (S_2V^{red}). Nitrogenase activity was determined from the decrease in absorbance at 600 nm upon addition of 0.4 µM of NifDK^{Av} and increasing concentrations of NifH^{Av} or *Sc*NifH^{Ht}. Absorbance was recorded using a USB 400-ISS-UV/VIS spectrophotometer (Ocean Optics) using a cuvette with a path length of 0.2 cm. Nitrogenase activity calculations were performed as previously described[21].

Nitrogenase activity determination by S_2V^{red} assay in 96-well microtiter plates. Nitrogenase activity determined by the S_2V assay were scaled down to 200 µl reaction volume to be performed in a 96-well microtiter plate. Except for during the optimization of the method, the assay was performed using a mixture of 2 µM NifH^{Av} and 0.05 µM NifDK^{Av} (corresponding to a NifH:NifDK ratio of 40:1). Other reaction conditions such as buffer composition, ATP regenerating mixture and S_2V^{red} concentration were identical to those described in the section above. The plate was prepared under anaerobic conditions inside a glovebox (Coy Laboratories) and sealed using PCR plate sealing films. Absorbance reading was performed using an absorbance plate reader (SPECTROstar Nano, BMG LABTECH) operating at 30 °C. The absorbance was recorded for 1 h, with measurements taken every 30 s. Nitrogenase activity calculations were performed in Excel (Microsoft) using an molar extinction coefficient of 9925 M^{-1} cm^{-1} at 600 nm[21], and a path length of 5 mm. The slope was calculated using the range in which the decrease in absorbance was linear, normally for at least 10 min. The final calculation can be expressed in simplified form as k_{obs} (s^{-1}) =|m|/ ((ε·l) · [NifDK^{Av}]), where |m| is the absolute value of the slope of the decrease in absorbance at 600 nm, ε is the molar extinction coefficient of S_2V^{red} at 600 nm in M^{-1} cm^{-1} (9925), l is the path length in cm (0.5) and [NifDK^{Av}] is the molar concentration of NifDK^{Av} in the assay (normally 0.05e^{-6}).

Nitrogenase activity determination by ARA. ARA were performed by combining isolated *Sc*NifH^{Xx} variants (2.2 µM) with pure NifDK^{Av} (0.055 µM) in an ATP regenerating mixture (1.23 mM ATP, 18 mM phosphocreatine disodium salt, 2.2 mM $MgCl_2$, 3 mM DTH, 40 µg/mL creatine phosphokinase in 100 mM MOPS pH 7.0). The final reaction volume was 400 µl in 9 ml sealed vials. Vials were flushed with argon before the injection of 0.5 ml acetylene. After 15 min of incubation at 30 °C, reactions were stopped by the addition of 100 µl of 8 M NaOH. Ethylene produced was detected and quantified using a gas chromatograph (GC-2014, Shimadzu) fitted with a flame ionization detector. The separation column was a Porapak N 80/100 column (G3591-80072, Agilent technologies), using pure N_2 as a column carrier gas (25 ml/min flow), and a mixture of H_2/air for the flame.

Oxygen sensitivity assays. *Sc*NifH^{Xx} samples and NifH^{Av} were passed through PD-10 desalting columns (GE Healthcare) equilibrated with 100 mM MOPS (pH 7.5) to remove DTH. Oxygen sensitivity was tested inside an anaerobic glovebox (Coy Laboratories) as previously described[31] with slight modifications. First, 2.5 ml of 17.4 µM NifH in 100 mM MOPS (pH 7.5) was prepared in a 13 ml sealed glass vial. The atmosphere in the headspace was exchanged for argon. Diluted NifH sample was removed (t_0) before pure O_2 was injected (0.2 atm final) using a 250 µl gastight syringe (Hamilton). The vial was incubated at room temperature with shaking (800 rpm) on a thermomixer (Eppendorf) with an adaptor for 13 ml vials. Air exposed NifH samples were removed after 1, 2, 5 and 10 min. Fifty ul was transferred to open 9 ml vials (three technical replicates) containing 150 µl of 100 mM MOPS (pH 7.5) supplemented with 4 mM DTH. Finally, 200 ul ATP mixture supplemented with 5 µg of NifDK^{Av} was added before nitrogenase activity was measured following the protocol for ARA as described above.

Data availability

The authors declare that the data supporting the findings of this study are available within the article, its supplementary information and data, and upon request.

Received: 23 February 2022; Accepted: 6 June 2022
Published online: 20 June 2022

References

1. Chapin, F. S., Matson, P. A. & Vitousek, P. *Principles of Terrestrial Ecosystem Ecology* 2nd edn, 529 (Springer Science & Business Media, 2011).
2. Erisman, J. W. *et al.* Nitrogen: Too much of a vital resource. *Sci. Brief* https://doi.org/10.13140/RG.2.1.3664.8163 (2015).

3. Mus, F., Alleman, A. B., Pence, N., Seefeldt, L. C. & Peters, J. W. Exploring the alternatives of biological nitrogen fixation. *Metallomics* **10**, 523–538. https://doi.org/10.1039/c8mt00038g (2018).
4. Oldroyd, G. E. & Dixon, R. Biotechnological solutions to the nitrogen problem. *Curr. Opin. Biotechnol.* **26**, 19–24. https://doi.org/10.1016/j.copbio.2013.08.006 (2014).
5. Curatti, L. & Rubio, L. M. Challenges to develop nitrogen-fixing cereals by direct nif-gene transfer. *Plant Sci.* **225**, 130–137. https://doi.org/10.1016/j.plantsci.2014.06.003 (2014).
6. Buren, S. & Rubio, L. M. State of the art in eukaryotic nitrogenase engineering. *FEMS Microbiol. Lett.* **365**, fnx274. https://doi.org/10.1093/femsle/fnx274 (2018).
7. Buren, S., Jimenez-Vicente, E., Echavarri-Erasun, C. & Rubio, L. M. Biosynthesis of nitrogenase cofactors. *Chem. Rev.* **120**, 4921–4968. https://doi.org/10.1021/acs.chemrev.9b00489 (2020).
8. Bulen, W. A. & LeComte, J. R. The nitrogenase system from *Azotobacter*: Two-enzyme requirement for N2 reduction, ATP-dependent H2 evolution, and ATP hydrolysis. *Proc. Natl. Acad. Sci. USA* **56**, 979–986. https://doi.org/10.1073/pnas.56.3.979 (1966).
9. Seefeldt, L. C., Hoffman, B. M. & Dean, D. R. Electron transfer in nitrogenase catalysis. *Curr. Opin. Chem. Biol.* **16**, 19–25. https://doi.org/10.1016/j.cbpa.2012.02.012 (2012).
10. Corbin, J. L. Liquid chromatographic-fluorescence determination of ammonia from nitrogenase reactions: A 2-min assay. *Appl. Environ. Microbiol.* **47**, 1027–1030. https://doi.org/10.1128/aem.47.5.1027-1030.1984 (1984).
11. Chalk, P. M. The strategic role of 15N in quantifying the contribution of endophytic N2 fixation to the N nutrition of non-legumes. *Symbiosis* **69**, 63–80. https://doi.org/10.1007/s13199-016-0397-8 (2016).
12. Herridge, D. F. & Giller, K. E. In *Working with Rhizobia* (eds Howieson, J. G. & Dilworth, M. J.) 187–220 (Australian Centre for International Agricultural Research, 2016).
13. Smercina, D. N., Evans, S. E., Friesen, M. L. & Tiemann, L. K. Optimization of the 15N2 incorporation and acetylene reduction methods for free-living nitrogen fixation. *Plant Soil* **445**, 595–611. https://doi.org/10.1007/s11104-019-04307-3 (2019).
14. Joe Hanus, F., Carter, K. R. & Evans, H. J. In *Methods in Enzymology* Vol. 69 (ed. Anthony, S. P.) 731–738 (Academic Press, 1980).
15. Simpson, F. B. & Burris, R. H. A nitrogen pressure of 50 atmospheres does not prevent evolution of hydrogen by nitrogenase. *Science* **224**, 1095–1097. https://doi.org/10.1126/science.6585956 (1984).
16. Seefeldt, L. C. *et al.* Reduction of substrates by nitrogenases. *Chem. Rev.* **120**, 5082–5106. https://doi.org/10.1021/acs.chemrev.9b00556 (2020).
17. Dilworth, M. J. Acetylene reduction by nitrogen-fixing preparations from *Clostridium pasteurianum*. *Biochim. Biophys. Acta* **127**, 285–294. https://doi.org/10.1016/0304-4165(66)90383-7 (1966).
18. Stewart, W. D., Fitzgerald, G. P. & Burris, R. H. In situ studies on N2 fixation using the acetylene reduction technique. *Proc. Natl. Acad. Sci. USA* **58**, 2071–2078. https://doi.org/10.1073/pnas.58.5.2071 (1967).
19. Shah, V. K. & Brill, W. J. Nitrogenase. IV. Simple method of purification to homogeneity of nitrogenase components from *Azotobacter vinelandii*. *Biochim. Biophys. Acta* **305**, 445–454. https://doi.org/10.1016/0005-2728(73)90190-4 (1973).
20. Haskett, T. L., Knights, H. E., Jorrin, B., Mendes, M. D. & Poole, P. S. A simple in situ assay to assess plant-associative bacterial nitrogenase activity. *Front. Microbiol.* **12**, 690439. https://doi.org/10.3389/fmicb.2021.690439 (2021).
21. Badalyan, A. *et al.* An efficient viologen-based electron donor to nitrogenase. *Biochemistry* **58**, 4590–4595. https://doi.org/10.1021/acs.biochem.9b00844 (2019).
22. Jiang, X. *et al.* Exploiting genetic diversity and gene synthesis to identify superior nitrogenase NifH protein variants to engineer N2-fixation in plants. *Commun. Biol.* **4**, 4. https://doi.org/10.1038/s42003-020-01536-6 (2021).
23. Vogtle, F. N. *et al.* Global analysis of the mitochondrial N-proteome identifies a processing peptidase critical for protein stability. *Cell* **139**, 428–439. https://doi.org/10.1016/j.cell.2009.07.045 (2009).
24. Buren, S., Jiang, X., Lopez-Torrejon, G., Echavarri-Erasun, C. & Rubio, L. M. Purification and *in vitro* activity of mitochondria targeted nitrogenase cofactor maturase NifB. *Front. Plant Sci.* **8**, 1567. https://doi.org/10.3389/fpls.2017.01567 (2017).
25. Gavini, N., Tungtur, S. & Pulakat, L. Peptidyl-prolyl cis/trans isomerase-independent functional NifH mutant of *Azotobacter vinelandii*. *J. Bacteriol.* **188**, 6020–6025. https://doi.org/10.1128/JB.00379-06 (2006).
26. Westermann, B. & Neupert, W. Mitochondria-targeted green fluorescent proteins: Convenient tools for the study of organelle biogenesis in *Saccharomyces cerevisiae*. *Yeast* **16**, 1421–1427. https://doi.org/10.1002/1097-0061(200011)16:15%3c1421::AID-YEA624%3e3.0.CO;2-U (2000).
27. Buren, S. *et al.* Biosynthesis of the nitrogenase active-site cofactor precursor NifB-co in *Saccharomyces cerevisiae*. *Proc. Natl. Acad. Sci. USA* **116**, 25078–25086. https://doi.org/10.1073/pnas.1904903116 (2019).
28. Lopez-Torrejon, G., Buren, S., Veldhuizen, M. & Rubio, L. M. Biosynthesis of cofactor-activatable iron-only nitrogenase in *Saccharomyces cerevisiae*. *Microb. Biotechnol.* **14**, 1073–1083. https://doi.org/10.1111/1751-7915.13758 (2021).
29. Georgiadis, M. M. *et al.* Crystallographic structure of the nitrogenase iron protein from *Azotobacter vinelandii*. *Science* **257**, 1653–1659. https://doi.org/10.1126/science.1529353 (1992).
30. Mayhew, S. G. The redox potential of dithionite and SO-2 from equilibrium reactions with flavodoxins, methyl viologen and hydrogen plus hydrogenase. *Eur. J. Biochem.* **85**, 535–547. https://doi.org/10.1111/j.1432-1033.1978.tb12269.x (1978).
31. Eady, R. R., Smith, B. E., Cook, K. A. & Postgate, J. R. Nitrogenase of *Klebsiella pneumoniae.* Purification and properties of the component proteins. *Biochem. J.* **128**, 655–675. https://doi.org/10.1042/bj1280655 (1972).
32. Eady, R. R. & Postgate, J. R. Nitrogenase. *Nature* **249**, 805–810. https://doi.org/10.1038/249805a0 (1974).
33. Lopez-Torrejon, G. *et al.* Expression of a functional oxygen-labile nitrogenase component in the mitochondrial matrix of aerobically grown yeast. *Nat. Commun.* **7**, 11426. https://doi.org/10.1038/ncomms11426 (2016).
34. Temme, K., Zhao, D. & Voigt, C. A. Refactoring the nitrogen fixation gene cluster from *Klebsiella oxytoca*. *Proc. Natl. Acad. Sci. USA* **109**, 7085–7090. https://doi.org/10.1073/pnas.1120788109 (2012).
35. Wang, L. *et al.* A minimal nitrogen fixation gene cluster from *Paenibacillus* sp. WLY78 enables expression of active nitrogenase in *Escherichia coli*. *PLoS Genet* **9**, e1003865. https://doi.org/10.1371/journal.pgen.1003865 (2013).
36. Wang, X. *et al.* Using synthetic biology to distinguish and overcome regulatory and functional barriers related to nitrogen fixation. *PLoS ONE* **8**, e68677. https://doi.org/10.1371/journal.pone.0068677 (2013).
37. Smanski, M. J. *et al.* Functional optimization of gene clusters by combinatorial design and assembly. *Nat. Biotechnol.* **32**, 1241–1249. https://doi.org/10.1038/nbt.3063 (2014).
38. Yang, J., Xie, X., Wang, X., Dixon, R. & Wang, Y. P. Reconstruction and minimal gene requirements for the alternative iron-only nitrogenase in *Escherichia coli*. *Proc. Natl. Acad. Sci. USA* **111**, E3718-3725. https://doi.org/10.1073/pnas.1411185111 (2014).
39. Yang, J., Xie, X., Yang, M., Dixon, R. & Wang, Y. P. Modular electron-transport chains from eukaryotic organelles function to support nitrogenase activity. *Proc. Natl. Acad. Sci. USA* **114**, E2460–E2465. https://doi.org/10.1073/pnas.1620058114 (2017).
40. Yang, J. *et al.* Polyprotein strategy for stoichiometric assembly of nitrogen fixation components for synthetic biology. *Proc. Natl. Acad. Sci. USA* **115**, E8509–E8517. https://doi.org/10.1073/pnas.1804992115 (2018).
41. Burén, S. *et al.* Formation of nitrogenase NifDK tetramers in the mitochondria of *Saccharomyces cerevisiae*. *ACS Synth. Biol.* **6**, 1043–1055. https://doi.org/10.1021/acssynbio.6b00371 (2017).
42. Ledbetter, R. N. *et al.* The electron bifurcating FixABCX protein complex from *Azotobacter vinelandii*: Generation of low-potential reducing equivalents for nitrogenase catalysis. *Biochemistry* **56**, 4177–4190. https://doi.org/10.1021/acs.biochem.7b00389 (2017).
43. Alleman, A. B., Mus, F. & Peters, J. W. Metabolic model of the nitrogen-fixing obligate aerobe *Azotobacter vinelandii* predicts its adaptation to oxygen concentration and metal availability. *mBio* **12**, e0259321. https://doi.org/10.1128/mBio.02593-21 (2021).

44. Segal, H. M., Spatzal, T., Hill, M. G., Udit, A. K. & Rees, D. C. Electrochemical and structural characterization of *Azotobacter vinelandii* flavodoxin II. *Protein Sci.* **26**, 1984–1993. https://doi.org/10.1002/pro.3236 (2017).
45. Deistung, J. & Thorneley, R. N. Electron transfer to nitrogenase. Characterization of flavodoxin from *Azotobacter chroococcum* and comparison of its redox potentials with those of flavodoxins from *Azotobacter vinelandii* and *Klebsiella pneumoniae* (nifF-gene product). *Biochem. J.* **239**, 69–75. https://doi.org/10.1042/bj2390069 (1986).
46. Chen, K. *et al.* Alteration of the reduction potential of the [4Fe-4S](2+/+) cluster of *Azotobacter vinelandii* ferredoxin I. *J. Biol. Chem.* **274**, 36479–36487. https://doi.org/10.1074/jbc.274.51.36479 (1999).
47. Aznar-Moreno, J. A., Jiang, X., Burén, S. & Rubio, L. M. Analysis of nitrogenase Fe protein activity in transplastomic tobacco. *Front. Agron.* https://doi.org/10.3389/fagro.2021.657227 (2021).
48. Poza-Carrion, C., Jimenez-Vicente, E., Navarro-Rodriguez, M., Echavarri-Erasun, C. & Rubio, L. M. Kinetics of Nif gene expression in a nitrogen-fixing bacterium. *J. Bacteriol.* **196**, 595–603. https://doi.org/10.1128/JB.00942-13 (2014).
49. Waite, C. J. *et al.* Resource allocation during the transition to diazotrophy in *Klebsiella oxytoca*. *Front. Microbiol.* **12**, 718487. https://doi.org/10.3389/fmicb.2021.718487 (2021).
50. Howard, K. S. *et al. Klebsiella pneumoniae nifM* gene product is required for stabilization and activation of nitrogenase iron protein in *Escherichia coli*. *J. Biol. Chem.* **261**, 772–778. https://doi.org/10.1016/s0021-9258(17)36161-6 (1986).
51. Roberts, G. P., MacNeil, T., MacNeil, D. & Brill, W. J. Regulation and characterization of protein products coded by the nif (nitrogen fixation) genes of *Klebsiella pneumoniae*. *J. Bacteriol.* **136**, 267–279. https://doi.org/10.1128/jb.136.1.267-279.1978 (1978).
52. Petrova, N., Gigova, L. & Venkov, P. Dimerization of *Rhizobium meliloti* NifH protein in *Saccharomyces cerevisiae* cells requires simultaneous expression of NifM protein. *Int. J. Biochem. Cell Biol.* **34**, 33–42. https://doi.org/10.1016/s1357-2725(01)00102-9 (2002).
53. Eseverri, A. *et al.* Use of synthetic biology tools to optimize the production of active nitrogenase Fe protein in chloroplasts of tobacco leaf cells. *Plant Biotechnol. J.* **18**, 1882–1896. https://doi.org/10.1111/pbi.13347 (2020).
54. Mistry, J. *et al.* Pfam: The protein families database in 2021. *Nucleic Acids Res.* **49**, D412–D419. https://doi.org/10.1093/nar/gkaa913 (2021).
55. Weits, D. A., van Dongen, J. T. & Licausi, F. Molecular oxygen as a signaling component in plant development. *New Phytol.* **229**, 24–35. https://doi.org/10.1111/nph.16424 (2021).
56. Koskela, E. V. & Frey, A. D. Homologous recombinatorial cloning without the creation of single-stranded ends: Exonuclease and ligation-independent cloning (ELIC). *Mol. Biotechnol.* **57**, 233–240. https://doi.org/10.1007/s12033-014-9817-2 (2015).
57. Gietz, R. D. & Schiestl, R. H. Quick and easy yeast transformation using the LiAc/SS carrier DNA/PEG method. *Nat. Protoc.* **2**, 35–37. https://doi.org/10.1038/nprot.2007.14 (2007).
58. Hill, H. D. & Straka, J. G. Protein determination using bicinchoninic acid in the presence of sulfhydryl reagents. *Anal. Biochem.* **170**, 203–208. https://doi.org/10.1016/0003-2697(88)90109-1 (1988).

Acknowledgements

This work was supported, in whole or in part, by the Bill & Melinda Gates Foundation (INV-005889). Under the grant conditions of the Foundation, a Creative Commons Attribution 4.0 Generic License has already been assigned to the Author Accepted Manuscript version that might arise from this submission. R.T.G. and J.B were supported by Biotechnology and Biological Sciences Research Council, grant award BB/P012574/1. LCS and AB were supported by U.S. Department of Energy, Office of Science, Basic Energy Sciences (BES) award DE-SC0010687 to LCS. LP-T was recipient of FPU16/02284 from Ministerio de Educación, Cultura y Deporte. XJ is recipient of a doctoral fellowship from Universidad Politécnica de Madrid. SM-M was recipient of Becas de Colaboración (998142) from Ministerio de Educación y Formación Profesional. We thank Amanda Mpofu for helping with DNA constructs.

Author contributions

L.P.-T., D.C., S.M.-M., A.B., R.T.G., X.J., G.L.-T. and S.B. carried out the experimental work. M.V. performed yeast fermentations. L.P.-T., X.J., R.T.G., L.C.S., J.B., S.B. and L.M.R. designed experiments, analyzed data, and wrote the manuscript.

Competing interests

The authors declare no competing interests.

Additional information

Supplementary Information The online version contains supplementary material available at https://doi.org/10.1038/s41598-022-14453-x.

Correspondence and requests for materials should be addressed to S.B. or L.M.R.

Reprints and permissions information is available at www.nature.com/reprints.

Publisher's note Springer Nature remains neutral with regard to jurisdictional claims in published maps and institutional affiliations.